Microchimica Acta (2026) 193:141
https://doi.org/10.1007/s00604-026-07866-2

RESEARCH

Selection of ssDNA aptamers targeting the serine protease SPSFQ of *Acinetobacter baumannii* and development of an electrochemical impedance spectroscopy-based ultrasensitive SPSFQ biosensor

Canan Özyurt[1] · Meltem Afşar[2] · Gözde Ülker[3] · Ezgi Man[3] · Serap Evran[3] · Mustafa Kemal Sezgintürk[2]

Received: 31 October 2025 / Accepted: 16 January 2026
© The Author(s) 2026

Abstract

Acinetobacter baumannii (*A. baumannii*) is a Gram-negative bacterium that creates an increasing burden on the healthcare system due to its ability to develop multidrug resistance. Sensitive, rapid and on-site detection of *A. baumannii*, which has been declared a critical priority pathogen by the World Health Organization, is of great importance. Today, secretory proteins of pathogenic organisms attract attention not only for their role in invasive processes but also as targets for early diagnosis. In this context, SPSFQ, a recently identified secretory protease, is a valuable target for the detection of *A. baumannii* at very low initial levels, before significant colonization occurs. In this study, ssDNA aptamers for SPSFQ were selected for the first time using the Systematic Evolution of Ligands by Exponential Enrichment (SELEX) method. The two aptamer sequences identified through SELEX were named Apt1 and Apt2, with Kd values of 42.10 ± 6.7 nM and 26.98 ± 1.35 nM, respectively. An ultrasensitive EIS-based biosensor was developed using Apt2, achieving a detection limit of 5.44 fg/mL and a linear range of 1.0–10,000 fg/mL. The aptasensor exhibited good repeatability (RSD: 2.62%) and reproducibility (RSD: 6.62%), and also maintained satisfactory stability during storage. Furthermore, the developed biosensor demonstrated reliable and remarkable performance in real commercial human serum samples, with recovery values of 110.84% and 104.40% for serum samples spiked with 250 and 6500 fg/mL SPSFQ, respectively.

Keywords Biosensor · Aptamer · SELEX · *Acinetobacter baumannii* · Electrochemical impedance spectroscopy

Introduction

Acinetobacter baumannii (*A. baumannii*), a Gram-negative, aerobic coccobacillus, is considered a significant pathogen in the modern healthcare system [1]. The versatile genetic structure of *A. baumannii*, one of the main causes of infections in hospitals and intensive care units, enables it to rapidly develop resistance mechanisms to harsh environmental conditions [2]. The importance of analyzing *A. baumannii*, classified as a "critical priority pathogen" by the World Health Organization, stems from several factors, primarily its multidrug-resistant nature. *A. baumannii* infections are common worldwide and are associated with high morbidity and mortality rates. These infections prolong hospital stays, place a heavy burden on healthcare systems, and complicate treatment [3]. Therefore, the accurate identification of *A. baumannii*, an understanding of its resistance mechanisms, and the development of effective treatment strategies are critical. Although traditional culture and biochemical methods are used for the detection of *A. baumannii*, these methods are time-consuming and often cannot definitively distinguish *A. baumannii* from phylogenetically similar species [4]. Molecular methods, particularly PCR-based assays and isothermal amplification techniques, have made significant advances by offering high sensitivity and

✉ Canan Özyurt
cananozyurt@comu.edu.tr

✉ Mustafa Kemal Sezgintürk
msezginturk@comu.edu.tr

[1] Department of Chemistry and Chemical Processing Technologies, Lapseki Vocational School, Çanakkale Onsekiz Mart University, Çanakkale, Türkiye

[2] Bioengineering Department, Engineering Faculty, Çanakkale Onsekiz Mart University, Çanakkale, Türkiye

[3] Department of Biochemistry, Faculty of Science, Ege University, İzmir, Türkiye

Published online: 07 February 2026

specificity [5]. However, these molecular tests often require specialized equipment and may have limited applicability in resource-poor regions. Detecting *A. baumannii* remains challenging, particularly because multidrug-resistant strains can lead to treatment delays. Despite these limitations, accurate and rapid diagnosis is critical for infection control and effective antibiotic stewardship [4]. Biosensors developed with different measurement strategies are very useful for the analysis of bacteria due to their superior sensitivity and specificity. A variety of optical and electrochemical biosensors have been designed for the detection of *A. baumannii* [6–8]. These biosensors generally rely on direct analysis of the bacteria or their DNA sequence. Although functional strategies for the detection of secretory proteins of other bacteria have been remarkably effective for early detection [9], a biosensor with this approach has not yet been developed for the detection of *A. baumannii*. Enzymes secreted by pathogens, particularly serine proteases, play a critical role in the interaction between microorganisms and their hosts and the progression of infection [10]. These enzymes are important determinants of pathogenicity and virulence, while also serving as potential biomarkers for diagnosing infections [11]. SPSFQ is an extracellular subtilisin-like serine protease recently isolated and characterized from *A. baumannii* [12]. Specific detection of SPSFQ enzyme holds great promise for indirect detection of *A.baumannii*. To the best of our knowledge, no recognition elements (neither antibodies nor aptamers) have been reported in the literature nor are they commercially available for this newly identified secretory protease. In this study, SPSFQ-specific ssDNA-based aptamers were selected for the first time by the magnetic bead-based systematic evolution of ligands by exponential enrichment (SELEX) method. The SELEX approach is a well-established method for the development of nucleic acid-based recognition elements with high specificity and selectivity against different targets. Nucleic acid aptamers are recognition elements that serve as strong alternatives to antibodies, offering advantages such as adaptability to environmental conditions, high chemical stability, and low production cost. In biosensor studies, the ability to chemically modify aptamers in different regions provides benefits in terms of both orientation and immobilization efficiency [13]. In this study, we developed two aptamer sequences (Apt1 and Apt2) using the MB-SELEX method, with Kd values of 42.10 ± 6.7 nM and 26.98 ± 1.35 nM, respectively. For SPSFQ detection, an electrochemical impedance spectroscopy (EIS)-based biosensor was designed using the 83-nucleotide Apt2 sequence. EIS is a label-free electrochemical technique that enables sensitive monitoring of interfacial changes occurring on the electrode surface upon target–recognition element interaction. Owing to its high sensitivity, non-destructive nature, and suitability for real-time measurements, EIS has been widely employed in aptamer-based biosensor platforms for protein and pathogen detection [14]. In this EIS-based study, ITO-PET electrodes, used as working electrodes, offer advantages over traditional electrodes due to their superior conductivity, ease of modification, low cost, large working surfaces, and environmental resistance. Within the scope of this study, an impedimetric biosensor was developed for the first time for SPSFQ detection using thiol-labeled aptamers, achieving sensitivity at the fg/mL level. The analytical performance characteristics of the biosensor were comprehensively characterized, and its potential application for SPSFQ detection in commercial human serum was evaluated.

Materials and methods

Chemicals and instrumentation

In the SELEX study, the ssDNA library (DAL-N-40 5' A GGAATTCAGATCTCCCTGCAG (N)40 CTCGAGGA GCTCAGGATCCCG (83 mer)) was constructed from a 40-nucleotide randomly selected region and purchased from Alpha Diagnostic Intl Inc. (USA). Ni-NTA magnetic agarose beads were supplied by Jena Bioscience (Jena, Germany). The consumables used in PCR studies were supplied by Thermofisher Scientific (Waltham, USA), agarose from Condalab (Madrid, Spain), lambda exonuclease from New England Biolabs (USA), and PCR clean-up kit from Macherey-Nagel (Düren, Germany). The ÄKTA prime protein purification system used for protein purification was purchased from GE Healthcare (Sweden), SDS-PAGE electrophoresis systems from Hoefer Pharmacia Biotech (USA), heater blocks (Biosan, Turkey), cooling-shaking incubators from New Brunswick Scientific (Enfield, USA), and UV transilluminator from Core Life Sciences (Laguna Niguel, USA). Other consumables were purchased from Sigma-Aldrich (Steinheim, Germany). The primers used in PCR studies were purchased from Sentegen (Ankara, Turkey) and Metabion (Martinsried, Germany), the thermal cycler from Applied Biosystems (California, USA), the agarose gel electrophoresis system from Hoefer Pharmacia Biotech (USA), and the Blue LED Illuminator for agarose gel imaging from Nippon Genetics Europe GmbH (Düren, Germany). Yeast extract, tryptone, ampicillin and agar for the preparation of agar plates used in cloning were purchased from Carl Roth GmbH (Karlsruhe, Germany). Growth media and the incubator in which the plates were incubated were supplied by New England Biolabs (Frankfurt am Main, Germany). The ultrasonicator for ultrasonic homogenization processes was supplied by Sonics (Newtown, CT, USA). The gene encoding the SPSFQ protein was synthesized by GenScript (New

Jersey, USA). Sanger sequencing analysis was performed at Sentebiolab (Ankara, Türkiye). For fluorescence characterization, FAM (6-carboxyfluorescein)-labeled aptamer candidates were purchased from Metabion (Martinsried, Germany). A Cary Eclipse Agilent (Santa Clara, USA) fluorescence spectrophotometer and a Thermo Scientific Microplate reader (Rockford, Illinois, USA) were used for fluorescence measurements. Gamry Reference 600 potentiostat/galvanostat (Gamry Instruments, Warminster, PA, USA) was used to perform EIS-based measurements. ITO sheets used as electrodes were supplied by Sigma-Aldrich (Steinheim, Germany). Scanning electron microscopy (SEM) and atomic force microscopy (AFM) measurements were carried out at Çanakkale Onsekiz Mart University Science and Technology Application and Research Center (Çanakkale, Türkiye).

Heterologous expression of the SPSFQ protein

The gene sequence encoding the *A. baumannii* SPSFQ protein was cloned into the pET-21a(+) vector and then transformed into *E. coli* BL21(DE3) cells, which served as expression hosts. For this purpose, chemically competent cells were prepared using the $RbCl_2$-based Hanahan protocol [15]. For the preparation of chemically competent cells, a single colony from LB-agar was inoculated into 5 mL LB broth, and 1 mL of the overnight culture was transferred into 100 mL LB medium. Cells were incubated at 37 °C until reaching an OD600 of 0.3–0.4, chilled on ice for 15 min, and harvested by centrifugation (4,000 rpm, 15 min, 4 °C). The pellet was resuspended in 20 mL of cold RF1 buffer, incubated on ice for 15 min, and centrifuged again under the same conditions. The resulting pellet was resuspended in 20 mL of RF2 buffer, incubated on ice for 15 min, and aliquoted (50 µL per tube). Competent cells were stored at − 80 °C. Buffer compositions are provided in Table S1. Then, the relevant plasmid DNA (50–100 ng) was added to the cell suspension, ensuring that the added DNA volume did not exceed 10% of the total competent cell suspension volume. After this step, incubations were performed sequentially for 30 min on ice, 30 s at 42 °C, and a second time for 2 min on ice. 200 µL of LB medium was added to the cell suspension and incubated at 37 °C for 1 h. Following incubation, the entire cell suspension was spread onto LB-Agar plates containing selective antibiotics. To initiate SPSFQ expression, a 2% (v/v) inoculum from the overnight culture was added to fresh LB medium, and SPSFQ protein was expressed following the protocol of Muhammed et al. [12]. Cell suspensions were centrifuged at 4000 rpm, 4 °C for 30 min, then washed twice with phosphate buffer (pH 7.4, 50 mM KH_2PO_4, 300 mM NaCl, 1% sarcosyl) and centrifuged under the same conditions. The cell pellet was resuspended in phosphate buffer (5 mL buffer per gram of cell pellet) and then ultrasonicated at 30% power for a total of 10 min to homogenize the sample. The insoluble fraction was separated from the supernatant by centrifugation at 13,000 rpm, 4 °C for 30 min. The clarified lysate (soluble fraction) was then purified using a GE Healthcare ÄKTA Prime chromatography system [16]. Since the pET21a(+) vector carries a 6xHis tag at the C-terminus, proteins were purified by immobilized nickel chelate affinity chromatography (IMAC) and bound to nickel magnetic agarose beads for future use in the SELEX step. For protein purification, a gradient was applied with a buffer containing 300 mM imidazole (pH 7.4, 50 mM KH_2PO_4, 300 mM NaCl, 300 mM imidazole) for elution. Before binding, magnetic beads were washed three times with Tris buffer (pH 7.5, 0.05% Tween 20). The clarified protein solution was added to the pre-washed Ni–NTA magnetic agarose beads and mixed (800 rpm, 25 °C, 30 min) to allow the His-tagged protein to bind. After incubation, the beads were washed three times with Tris buffer and then resuspended. Protein amounts were determined by the Bradford method [17]. Both free-form and magnetic bead-immobilized proteins were stored at 4 °C.

SDS-PAGE verification of Recombinant SPSFQ protein expression

Buffers used for the SDS-PAGE system are given in Table S2, and solutions used to prepare 12.5% SDS-PAGE gels are given in Table S3. SDS-PAGE gels were prepared according to the protocols in these Table [18]. Protein samples were mixed with SDS-PAGE sample buffer and incubated at 95 °C for 10 min. A final volume of 5 µL was applied to the gels and run for approximately 30 min at 50 mA, 300 V. Following the run, the gels were stained with Coomassie staining solution (0.2% (w/v) Coomassie Brilliant Blue G250, 50% (v/v) ethanol, and 10% (v/v) acetic acid) for 30 min with stirring, and the dye was removed by washing.

Keratinolytic activity test for SPSFQ protein

The keratinolytic activity of purified SPSFQ protein was determined using keratin azure K 8500 as a substrate and following a standard keratinase assay protocol (Sigma Aldrich). Keratin azure K 8500 was chosen as the substrate to determine the keratinolytic activity of purified SPSFQ because of the ability of keratinolytic enzymes to effectively degrade keratin proteins [12]. The standard keratinase activity determination protocol provided by Sigma Aldrich was developed to obtain reproducible results and allow comparison between different studies. Therefore, this method was used to determine the keratinolytic activity of SPSFQ. The

reaction mixture for the keratin degradation assay was prepared containing 20 mg of keratin azure, 4 mL of 50 mM sodium phosphate solution, and 1 µM purified SPSFQ sample. The keratinolytic reaction was incubated at 37 °C for 1 h to allow color development. Degradation of the modified substrate was quantitatively recorded by measuring the absorbance at 595 nm using proteinase K as a standard. One unit of keratinolytic activity is defined as the amount of enzyme required to increase the absorbance at 595 nm by 0.01 in 1 h at 37 °C. In this context, the enzymatic activity of the recombinant SPSFQ protein was confirmed.

MB-SELEX-based selection of SsDNA aptamers for SPSFQ protein

In vitro aptamer selection against SPSFQ protein was performed by applying 7 consecutive rounds of magnetic bead-based SELEX under varying conditions. In the SELEX study, pH 7.5 Tris buffer (containing 0.05% Tween 20) was used as the binding buffer. A total of an 83-nucleotide ssDNA library containing a 40-nucleotide random region was used in the SELEX process. Before the first SELEX round, 100 pmol of the ssDNA library was folded by incubating at 95 °C for 5 min, on ice for 5 min, and at 25 °C for 5 min. Then, negative SELEX was performed by treating with empty nickel beads and magnetic separation to remove ssDNA sequences that tended to bind to the beads. For the first SELEX round, 300 pmol of SPSFQ protein (on Ni-coated beads) was incubated with the unbound ssDNA library (from the negative selection step) for 2 h at 25 °C. After incubation, three washing steps were performed with binding buffer. The bound sequences were then eluted by incubating at 80 °C for 15 min and amplified by PCR. In the first SELEX round, 0.1 mg/mL bovine serum albumin (BSA) and 0.025 mg/mL salmon sperm DNA were added to the binding buffer containing ssDNA sequences that do not bind to the magnetic bead to mask potential nonspecific interactions in the next round. The dsDNA product obtained after PCR was treated with lambda exonuclease to obtain ssDNA. Thus, the first round of SELEX was successfully completed.

Figure 1 shows the general flowchart of the applied magnetic bead based SELEX method. Unless otherwise stated, a negative SELEX step was performed before each SELEX round, similar to the first round. The second SELEX round was concluded with the same procedures as the first round,

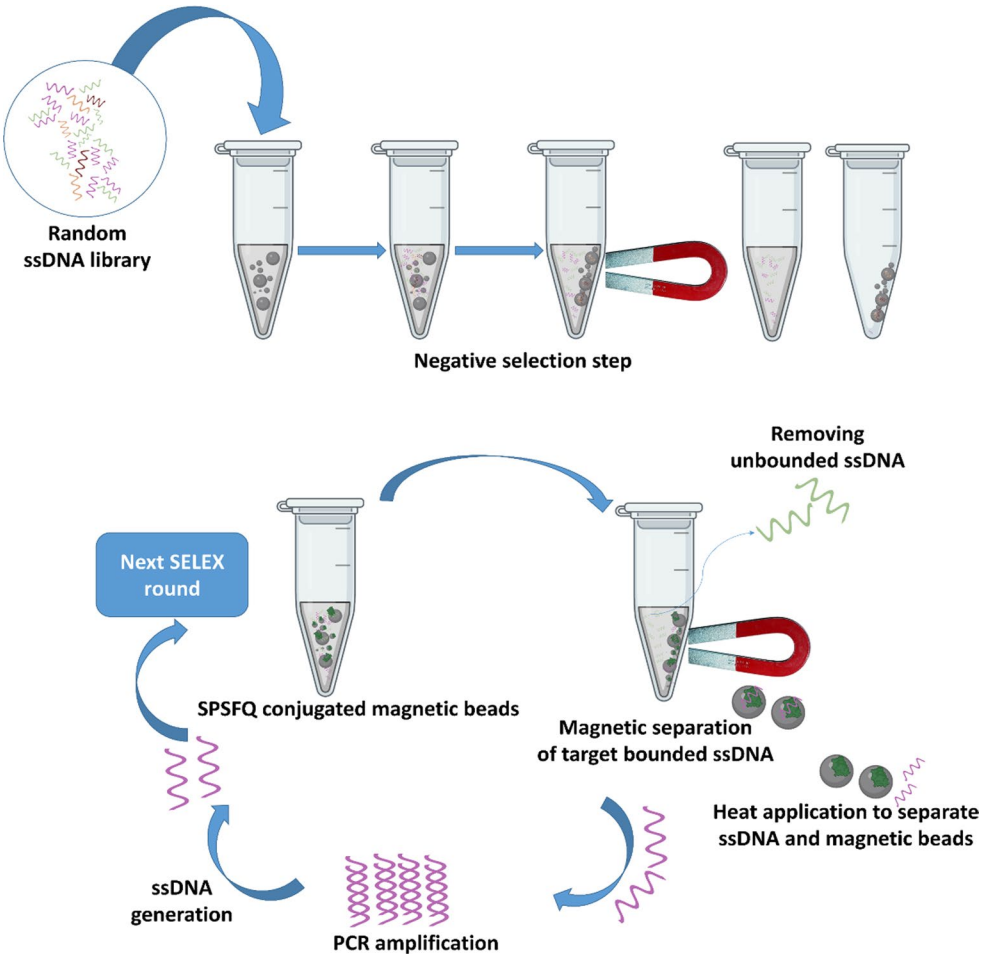


Fig. 1 General flow chart of the magnetic bead based SELEX method used to select ssDNA aptamers for SPSFQ protein

by reducing the amount of SPSFQ protein to 200 pmol. In the third SELEX round, the ssDNA library obtained from the second SELEX round was incubated with 150 pmol of SPSFQ protein for 90 min, and the process was completed similarly to the first round. Throughout the SELEX rounds, protein amounts and incubation times were reduced. The changing parameters during the SELEX process are listed in Table S4.

Polymerase chain reaction (PCR) protocol and lambda exonuclease digestion

PCR was performed with an initial denaturation of 5 min at 95 °C, followed by at least eight cycles of 30 s at 95 °C, 30 s at 64 °C, and 30 s at 72 °C. The number of cycles was initially set at eight to prevent nonspecific band formation and increased as needed after agarose gel analysis. The dsDNA, confirmed to be pure by gel analysis, was eluted using a PCR purification kit and subsequently treated with lambda exonuclease to generate ssDNA for the next SELEX round [19]. Lambda exonuclease is a 5′ to 3′ exonuclease that selectively cleaves 5′-phosphorylated DNA strands. In PCR stage, one strand of dsDNA was phosphorylated using a 5′-phosphorylated reverse primer, and ssDNA was obtained after enzyme incubation. For this purpose, 5 µg of dsDNA was incubated with 5 units of enzyme in a 50 µL reaction mixture at 37 °C for 30 min, followed by inactivation of the enzyme at 75 °C for 10 min. The concentration of ssDNA purified with the isolation kit was determined by microplate spectrophotometer (260 nm) and confirmed on agarose gel.

Monitoring sequence enrichment by real-time polymerase chain reaction (RT-PCR)

Tm analysis was performed by real-time PCR to monitor DNA enrichment during SELEX cycles [20]. Approximately 10 ng of PCR product from each cycle was prepared in a total volume of 20 µL using the iTaq SYBR Green kit. For post-amplification melting curve analysis, reactions were heated from 40 °C to 95 °C at 0.7 °C/min. Fluorescence changes were continuously monitored and melting points were calculated by the instrument software. Based on the Tm analysis results, the SELEX process was completed in the 7th cycle.

Structural homology analysis of aptamer candidates and determination of their secondary structures

After the seventh round of SELEX, samples were subjected to sequence analysis. The resulting chromatograms were processed using the UGENE software, and homology analysis was performed with the MEME Suite [21]. Based on MEME Suite results, two families with high sequence homology were identified, and the resulting aptamer candidates were designated as Apt1 and Apt2. The secondary structures of these aptamers were further analyzed using the Mfold web server [22].

Determination of dissociation constant (Kd) values of aptamers

Aptamer candidates were ordered with FAM labels, and Kd values were determined for both aptamer candidates using differences in fluorescence intensity. To determine the Kd values of the respective aptamers, the FAM-labeled aptamer sequences were first folded independently in binding buffer. For this purpose, the aptamers were incubated at 80 °C for 10 min, on ice for 10 min, and at 25 °C for 10 min. Aptamers at a final concentration of 0.1 µM were incubated with increasing concentrations (between 25 and 126 nM) of SPSFQ protein immobilized on magnetic beads for 30 min at 25 °C. Following incubation, bound sequences were removed by applying a magnetic field. The fluorescence intensity of the unbound fraction was compared with the fluorescence intensity of the blank sample (containing 0.1 µM aptamer), and the fluorescence difference was calculated. The Kd values of the aptamers were determined using the single-site binding model "Hill-curve binding function" with the Graph Pad Prism 5.01 program [23].

Configuration of EIS-based aptasensor

EIS and cyclic voltammetry (CV) are reliable methods for evaluating the analytical performance of biosensors and the interface properties of electrode surface modifications. Because protein accumulation restricts electron and mass transport, increasing analyte concentrations led to significant changes in surface insulation. The Rct values associated with SPSFQ concentrations were used as key parameters in optimization and performance analyses. The linear response determined by the equivalent circuit model (Rs, Zw, Rct) was confirmed, particularly by the changes in Rct, which reflect the double-layer capacitance [24]. The accumulation on the electrode surface following the SPSFQ–aptamer interaction was monitored in relation to the changes in Rct for the potassium ferricyanide/ferrocyanide redox couple. The impedance spectra were evaluated using a standard Randles equivalent circuit model, which is widely applied in impedimetric biosensor studies. The charge transfer resistance (Rct) values were obtained by fitting the experimental Nyquist plots to the equivalent circuit, where Rct corresponds to the diameter of the semicircle in the high-frequency region.

For modification of ITO-PET electrodes with ssDNA aptamer, the surfaces were first cleaned and activated with OH groups. During cleaning, the electrodes were ultrasonicated separately in acetone, soap solution, and ultrapure water for 10 min each. Then, the electrodes were incubated in $NH_4OH/H_2O_2/H_2O$ (1:1:5, v: v:v) solution for 90 min. The electrochemical properties of the modified electrodes were evaluated by CV and EIS; a redox probe solution containing 5 mM $[Fe(CN)_6]^{4-}$, 5 mM $[Fe(CN)_6]^{3-}$, and 0.1 M KCl was used in the measurements. OH-activated ITO-PET electrodes were incubated with 3-aminopropyltriethoxysilane (3-APTES) overnight (prepared as 1% and 2% v/v in ethanol during the optimization steps). Changes in surface conductivity after 3-APTES modification were evaluated by CV and EIS measurements. Then, the electrodes were incubated with sulfosuccinimidyl 4-(N-maleimidomethyl) cyclohexane-1-carboxylate (sulfo-SMCC) for 2 h, and CV and EIS analyses were performed. Sulfo-SMCC modification provided a surface composition suitable for binding of thiol-modified aptamers. For aptamer immobilization, 5′-SH-$(CH_2)_6$ modified aptamers were folded by incubating in binding buffer containing 10 mM TCEP for 5 min at 95 °C, 5 min on ice, and 5 min at room temperature. This process was performed to ensure the formation of the secondary structure necessary for the interaction with the SPSFQ protein. Folded aptamers were immobilized onto sulfo-SMCC-modified electrodes by incubation for 1 h. Then, CV and EIS measurements were recorded to confirm aptamer immobilization. In the final step, blocking was performed by incubation with 6-Mercapto-1-hexanol (6-MCH) for 30 min. Changes in surface conductivity and electron transfer after 6-MCH blocking were confirmed by CV and EIS. Optimization studies were performed by impedimetrically analyzing the binding capacities of the functional electrodes with different SPSFQ concentrations.

Surface characterization of biosensor

SEM and AFM techniques were used to characterize the surface morphology of the SPSFQ aptasensor at different immobilization stages. AFM measurements were performed in non-contact mode over a 5 × 5 μm area. SEM and AFM images of the modified surfaces at each stage were recorded and evaluated. Surface morphologies were also evaluated using the roughness data obtained from the AFM measurements.

Optimization of aptasensor performance parameters

The following equation was used for all protein measurement steps for the SPSFQ aptasensor:

$$\triangle Rct = Rct\,(SPSFQ) - Rct\,(MCH)$$

In this equation, ΔRct represents the change in charge transfer resistance resulting from SPSFQ binding, Rct(SPSFQ) represents the charge transfer resistance obtained after the addition of SPSFQ, and Rct(MCH) represents the charge transfer resistance obtained during the last modification step with 6-MCH.

Biosensor optimization was performed by systematically varying the concentrations of 3-APTES, sulfo-SMCC, and aptamers, while keeping all other parameters constant (Table S6). For silanization, OH-activated ITO-PET electrodes were incubated overnight with 1% or 2% (v/v) 3-APTES in ethanol, and the effect on surface properties and protein recognition was evaluated by EIS in the 1.0 fg/mL–10,000 fg/mL SPSFQ concentration range. To optimize crosslinker density, electrodes were modified with 0.05, 0.1, or 0.2 mM sulfo-SMCC, and impedimetric responses were recorded following 1 h protein incubation. Finally, aptamer immobilization was assessed using 0.5 μM and 1 μM aptamer solutions. CV and EIS measurements were conducted to determine the effect of aptamer concentration on biosensor performance across the same analyte range.

Analytical characterization of the biosensor

Construction of the linear calibration curve

Optimization parameters were used to generate the linear calibration curve for the aptamer-based EIS biosensor. A calibration curve was created using the changes in Rct values generated by SPSFQ protein at each concentration in the range of 1.0–10,000 fg/mL, using triplicate runs. The calibration curve was created by plotting the ΔRct values obtained from EIS measurements against SPSFQ concentration.

Reproducibility studies

Since reproducibility is a key factor for biosensors, the reproducibility of the aptasensor was evaluated using linear plots of 10 individual curves, all configured under the same optimized conditions. SPSFQ protein was applied to each biosensor in the concentration range of 1.0–10,000 fg/mL and linear calibration plots were obtained. Relative standard deviation (% RSD) was calculated for the slopes from the overlapping line plots.

Repeatability studies

For repeatability studies, 10 different electrodes were prepared identically. 2000 fg/mL SPSFQ protein was applied

to each prepared electrode independently. The ΔRct values obtained for each electrode were calculated using the equation of the calibration chart, and the corresponding concentration values were calculated. Based on the obtained data, the coefficient of variation (%CV) was calculated.

Determination of limit of detection (LOD) and limit of quantification (LOQ) values

The Eq. 3 σ/m and 10 σ/m were used to calculate LOD and LOQ values, respectively. In these equations, σ is the standard deviation of blank measurements, and m is the slope of the calibration graph. For this purpose, the mean and standard deviation of the ΔRct values recorded from 10 blank measurements (electrodes treated with binding buffer only) were calculated.

Determination of biosensor selectivity

To determine biosensor selectivity, potential interferents haptoglobin, ascorbic acid, and glucose, and a mixture of these three molecules, were applied independently with SPSFQ protein at a final concentration of 250 fg/mL each. The ΔRct value obtained for SPSFQ protein alone at 250 fg/mL was assumed to be 100, and the percent interference values of the respective interferents were determined in the presence of SPSFQ. Accordingly, the selectivity of the sensor was evaluated.

Determination of SPSFQ protein in commercial human serum samples

Real human serum (commercially available from Merck with product code: H4522), was used as the serum sample. For this purpose, the serum was diluted 1000-fold with the working buffer. This value was determined considering the absence of SPSFQ protein in the serum of a healthy individual, minimizing the matrix effect, and considering the sensor's dynamic range. First, the modified ITO-PET electrodes were incubated with the diluted serum sample for 1 h, and the matrix effect of the serum was determined using the ΔRct value. This value was subtracted from the signals obtained in subsequent experiments and calculations were made. Different serum samples at the same dilution were independently treated with standard additions of 250 and 6500 fg/mL SPSFQ protein, respectively. Triplicate runs were performed for each concentration, and the measured concentrations were determined using the equation of the calibration curve using the average values. The measurement performance in serum was evaluated using the obtained values. For this purpose, RSD % values were determined by dividing the standard deviation values obtained in triplicate measurements by the average value calculated in triplicate measurements and multiplying by 100 (% RSD =(σ/m)X100)). % Recovery values were calculated by taking the ratio of the measured value (concentration calculated from the calibration graph) to the actual value added (% recovery=[Calculated concentration (fg/mL)/Added concentration (fg/mL)]x100).

Determination of biosensor storage stability

Weekly measurements were taken for a single analyte concentration (2000 fg/mL) with different electrodes prepared on the same day under optimized conditions.

Results and discussion

Heterologous expression and activity analysis of the SPSFQ protein

After successful heterologous expression of the SPSFQ protein, the concentration of the resulting recombinant protein was determined quantitatively using the Bradford protein assay [17]. The SPSFQ recombinant protein was obtained at a concentration of approximately 1 mg/mL. This concentration demonstrates that the heterologous expression process was highly efficient and that the targeted recombinant protein was successfully produced in sufficient quantities for subsequent applications.

SDS-PAGE analysis of SPSFQ protein

The purity of the recombinant SPSFQ protein was confirmed by SDS-PAGE. A protein band with a molecular weight of approximately 38 kDa was obtained, as expected [12]. This result demonstrates that the recombinant SPSFQ protein was expressed, and that it was successfully purified by metal-chelate affinity chromatography. The gel image of the protein, whose purity was determined by SDS-PAGE, is shown in Fig. 2A.

Keratinolytic activity test results for SPSFQ

The active form of the recombinant SPSFQ protein was demonstrated by a 0.05 increase in absorbance for 1 μM purified SPSFQ protein using Keratin Azure K 8500. The color change (corresponding to a 5 unit increase in SPSFQ) for proteinase K and recombinant SPSFQ proteins used as controls for the respective reaction is shown in Fig. 2B. One unit of keratinolytic activity is defined as the amount of enzyme required to increase the absorbance at 595 nm by 0.01 in 1 h at 37 °C [12]. Based on this calculation, SPSFQ

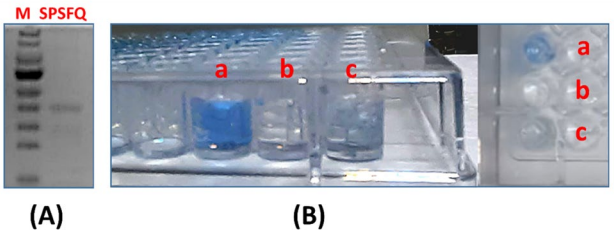


Fig. 2 **(A)** SDS-PAGE image of purified SPSFQ protein. (M; "Thermo Scientific PageRuler Prestained Protein Ladder" protein marker, molecular weights are 180, 130, 100, 70, 55, 40, 35, 25, 15, 10 kDa, respectively). **(B)** a: Proteinase K standard, b: Buffer, c: Color change reaction corresponding to 5 unit enzyme activity at 595 nm for SPSFQ protein

activity corresponds to a value of approximately 5 units. Based on the results, it was determined that the recombinant SPSFQ protein possesses proteolytic activity and that the enzyme was expressed in its active form. Confirmation of enzymatic activity is essential because, without this validation, the protein cannot be considered a reliable target for aptamer development. In this study, the enzymatic activity of SPSFQ was successfully demonstrated, ensuring that the recombinant protein retains its native functionality and is therefore suitable for subsequent biosensor applications.

Selection of SsDNA aptamers for SPSFQ protein by MB-SELEX method

The findings obtained from the SELEX cycles are presented in Table S5. In the first SELEX round, a DNA band was first detected after 18 PCR cycles; this required cycle number decreased in later rounds, reaching 12 cycles in the final round. This decrease in required PCR cycles indicates successful enrichment of target-binding sequences. Images of the PCR products obtained through agarose gel electrophoresis over the seven rounds are shown in Fig. 3A. Gel images of the ssDNA sequences obtained for each round following the reaction with lambda exonuclease are shown in Fig. 3B. Agarose gel visualization of ssDNA sequences corresponding to approximately 40 bases revealed the formation of a clear single band, and the resulting ssDNA sequences were used in the next SELEX round. Since the SELEX cycle was terminated at the 7th round, no cleavage reaction was performed after this round. The products obtained after the reaction with lambda exonuclease were isolated using the Macherey-Nagel PCR-clean-up kit, and their concentrations were measured spectrophotometrically at 260 nm (Table S5).

Monitoring sequence enrichment with RT-PCR

Visualizing and verifying ssDNA production from PCR products using traditional methods appears insufficient for the initial rounds of aptamer SELEX. This inadequacy stems from the presence of over 10^{15} different sequences in the preliminary library. Verifying ssDNA production is a crucial step in the SELEX process. This is because ssDNA must be able to form a suitable three-dimensional structure that allows it to bind to the target of interest with high affinity and specificity. Real-time PCR and melting curve analysis are known to distinguish single-stranded DNA (ssDNA) and double-stranded DNA (dsDNA) in their presence based on their respective melting temperatures (Tm) [20]. As seen

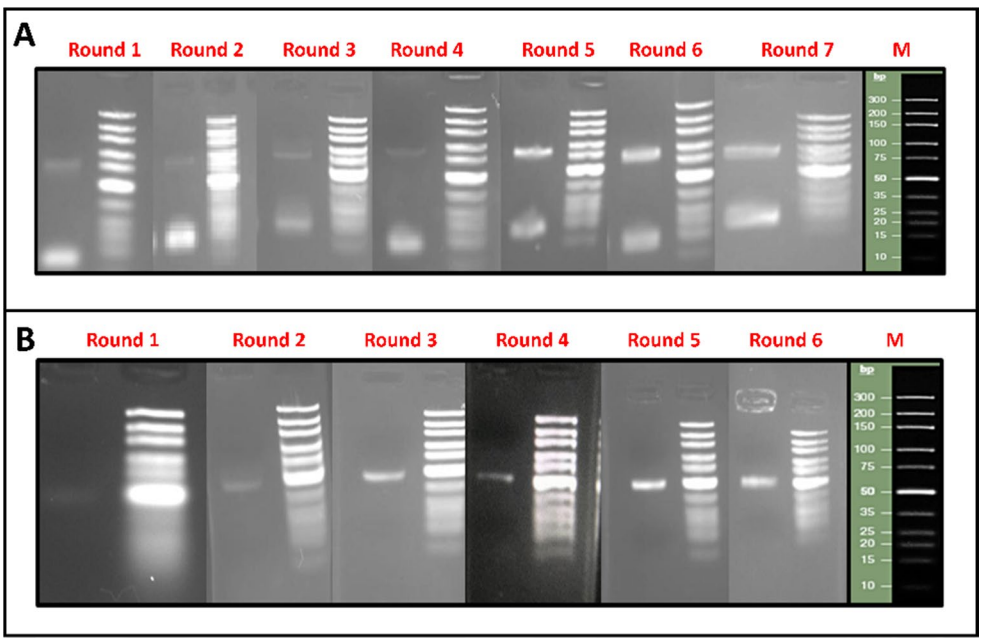


Fig. 3 **(A)** Agarose gel electrophoresis images of dsDNA sequences obtained after PCR during SELEX rounds, **(B)** Agarose gel image of ssDNA after digestion with lambda exonuclease (DNA marker: Thermo Scientific, GeneRuler Ultra Low Range DNA Ladder, SM1211)

in Fig. S1, the Tm value showed a significant increase in Round 7. This increase confirms enrichment.

Structural homology analysis of aptamer sequences and determination of their secondary structures

Multiple sequence alignment was performed to identify subsequences enriched among aptamer sequences. The MEME-suite program was used to determine the frequency of similar sequences among aptamer sequences and to perform motif analysis. According to the results of the MEME-suite program, enrichment was detected in two different motifs. The consensus sequences obtained using this program represent the forward and reverse log odds ratio. The log odds ratio is the logarithm of the ratio of the probability of occurrence of motifs given in the motif model to the background model probability, and high values are interpreted as a positive parameter [21]. According to the MEME suite analysis, two main families and two different consensus sequences were found. The p-values of the order of 10^{-18} obtained in the SELEX study are extremely small (essentially close to zero). This indicates an extremely high level of statistical significance. The interpretation of this p-value indicates that the probability of the discovered DNA motif occurring by chance alone is very low. Instead, it suggests that the motif is likely biologically significant and represents a specific binding pattern within the selected ssDNA ligands. The smaller the p-value, the stronger the evidence supporting the significance of the discovered motif [21]. Table S7 shows the sequences of aptamer candidates identified with the MEME suite. Sequences highlighted in red represent primer binding sites, and underlined sequences represent random sequences. The online Mfold program was used to identify secondary motifs enriched in aptamer sequences. The secondary structures with the lowest Gibbs free energy predicted by the Mfold web server for the two aptamer candidates are presented in Fig. 4, with Apt1 shown in Fig. 4A and Apt2 in Fig. 4B. Folding conditions for aptamer secondary structure prediction were determined as 100 mM Na^{+}, 2 mM Mg^{2+}, and 25 °C. Advanced fluorescence characterization was performed on the aptamers whose sequences and secondary structure analyses were determined.

Two of the candidates, whose probable secondary structures were determined using the Mfold method, had negative ΔG° values, indicating stable folding and secondary structure formation. Both structures contain stem-loop motifs. These motifs are common secondary structural components of ssDNA and play important roles in the molecule's specific functions, such as target binding.

Determination of aptamer Kd values

The binding affinities of 5′-FAM-labeled Apt1 and Apt2 were tested at 25 °C. An increase in fluorescence intensity

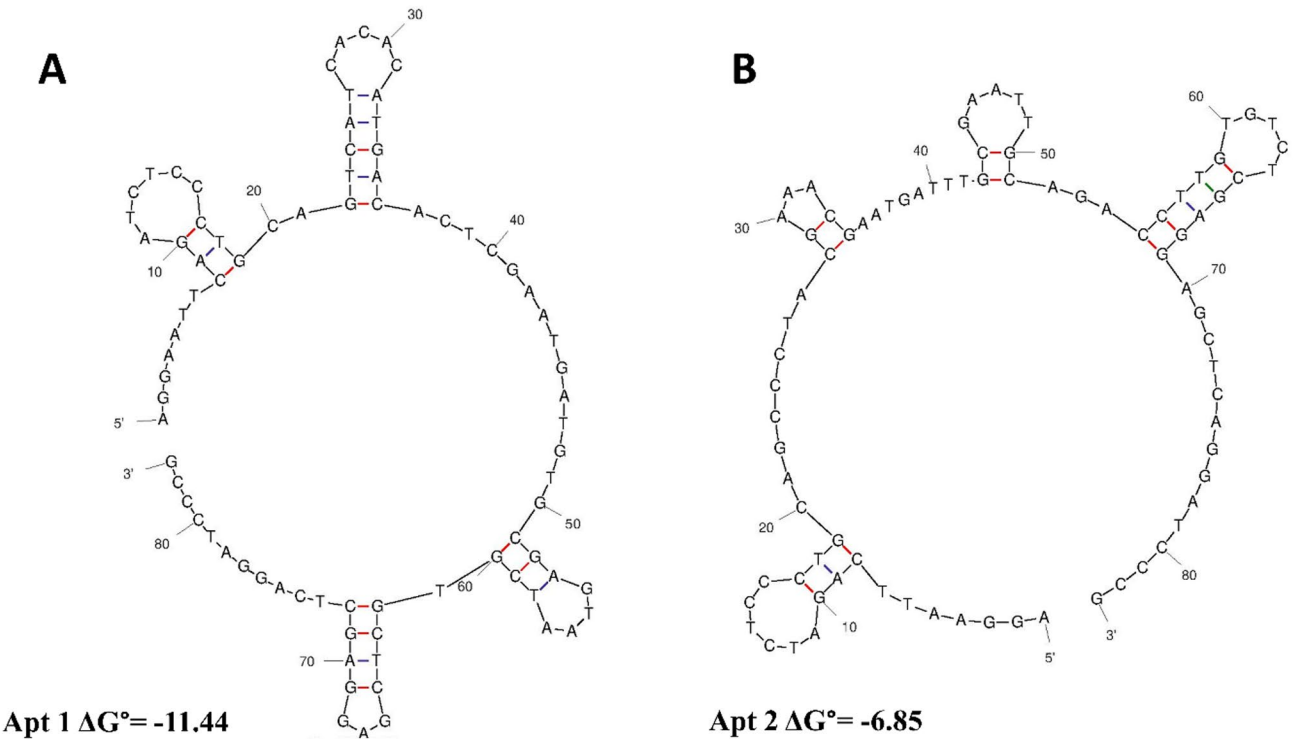


Fig. 4 Secondary structures predicted by the Mfold web server for (**A**) Apt1 and (**B**) Apt2

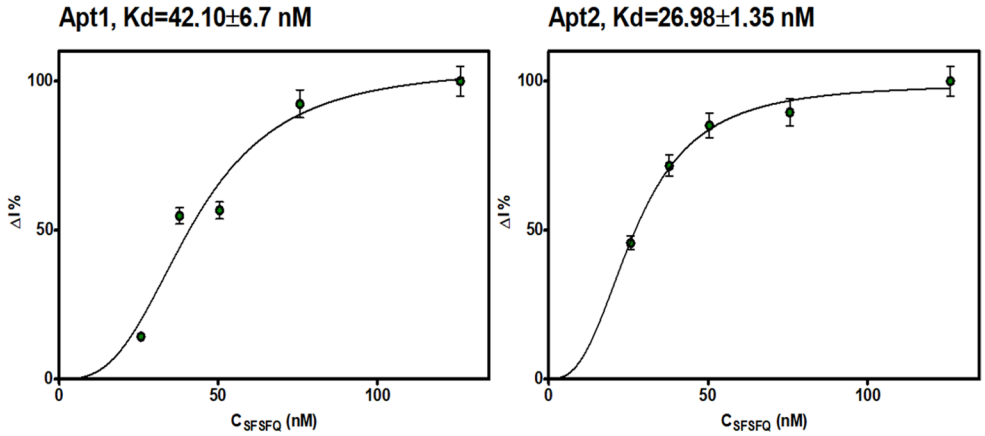


Fig. 5 Single-site binding model (Hill-curve binding) graphs obtained after incubation of Apt1 and Apt2 with increasing concentrations of SPSFQ protein

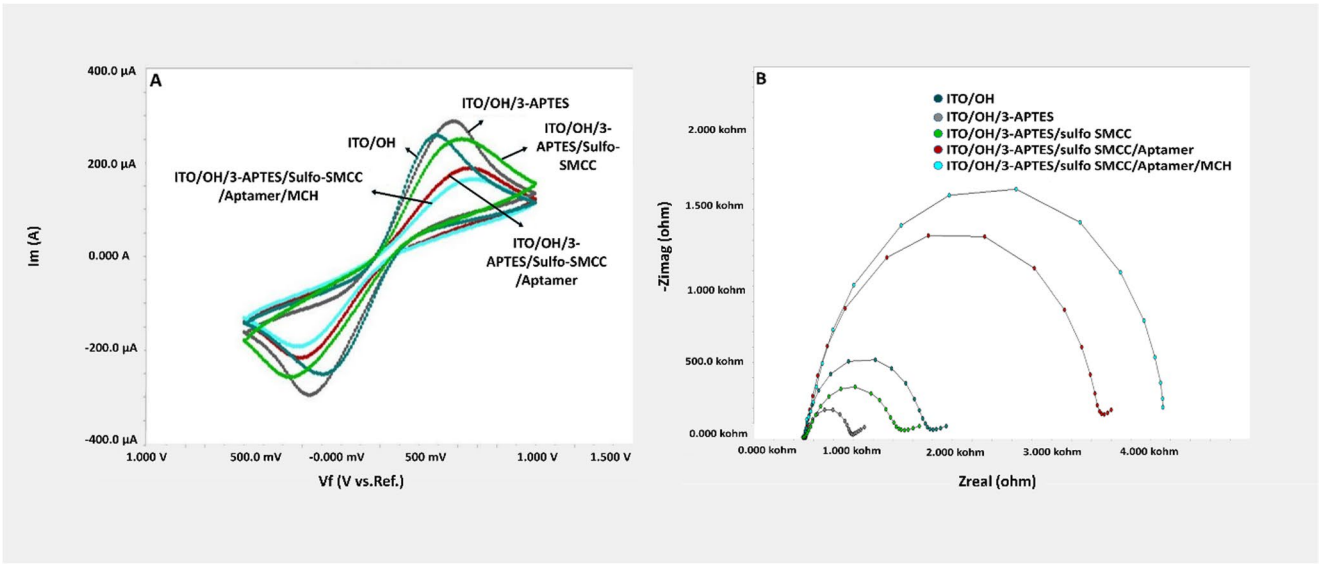


Fig. 6 **A**) CV diagrams and **B**) EIS spectra of the immobilization stages of the developed biosensor

was observed with increasing amounts of bound sequences along with increasing protein concentrations. Saturation was determined for both aptamers at a concentration of 126 nM SPSFQ protein. The Kd value for Apt1 was determined to be 42.10 ± 6.7 nM, and for Apt2, 26.98 ± 1.35 nM (Fig. 5). The lower Kd value of Apt2 suggests that Apt2 binds to SPSFQ with slightly higher affinity than Apt1. Both aptamer candidates exhibit high binding affinities with Kd values in the nM range.

Initial tests indicated that Apt2 offered higher reproducibility and a better linear relationship between signal and analyte concentration. Therefore, the Apt2 aptamer was used in subsequent studies. The Kd values obtained for SPSFQ aptamers are similar to the binding affinities of aptamers developed against proteins and bacteria of bacterial origin in the literature [25]. To the best of our knowledge, no recognition elements — not even antibodies — have been reported in the literature or are commercially available for detecting the SPSFQ protein. Therefore, the aptamers developed in this study represent the very first recognition elements (and indeed the first aptamers) specific to the SPSFQ protein.

Modification of ITO-PET electrode surfaces with ssDNA aptamer

Each modification step of the electrodes modified as described in the method section was confirmed with CV (Fig. 6A.) and EIS (Fig. 6B.) measurements. In order to modify the surfaces of ITO-PET electrodes with ssDNA aptamer, first the surfaces of ITO-PET electrodes were activated with OH groups. Figure 6B shows the impedance values in the Nyquist plot for the ITO-PET/OH phase. After this phase, the electrode surface was incubated with 3-APTES overnight, and after modification, a noticeable decrease in the impedance value of the electrode surface occurred. CV measurements also confirmed the increase in surface conductivity after 3-APTES application. The observed result can be attributed to the interaction between

the positively charged amino group of the 3-APTES molecule and the negatively charged redox probe, indicating that electron transfer at the electrode surface is facilitated. The increase in CV anodic and cathodic peak currents after 3-APTES binding indicates an enhanced electron transfer rate at the electrode-electrolyte interface due to the addition of amino groups, potentially facilitating redox reactions or improving charge transfer kinetics. Following this step, CV and EIS measurements were performed for electrodes incubated with sulfo-SMCC for 2 h. Sulfo-SMCC is a heterobifunctional crosslinker containing N-hydroxysuccinimide (NHS) ester and maleimide groups, which allows covalent conjugation of amine and sulfhydryl-containing molecules. NHS esters react with primary amines at pH 7.0–9.0 to form amide bonds. The reaction of sulfo-SMCC's NHS esters with amine groups derived from 3-APTES alters the surface properties, leading to an increase in impedance. This change can be attributed to the modification of the electrode-electrolyte interface, affecting charge transfer and creating barriers that impede electron flow. CV measurements also confirm the change in surface conductivity. The aforementioned electrochemical mechanisms restrict the kinetics of redox reactions, leading to a decrease in the peak currents observed during anodic and cathodic scans in CV measurements. Sulfo-SMCC-modified electrodes were suitable for binding thiol-modified aptamers. For this purpose, aptamers were first folded in buffer at 95 °C for 5 min, on ice for 5 min, and at room temperature for 5 min. The folding process allowed the aptamers to form a secondary structure that would allow them to interact with their analyte, the SPSFQ protein. Following folding, the aptamers were immobilized on sulfo-SMCC-modified electrodes by incubation for 1 h. Sulfo-SMCC presents maleimide groups that react with thiol (-SH) groups. The stable covalent bond formed between the maleimide group of sulfo-SMCC and the thiol group of the aptamer results in the immobilization of the aptamer on the electrode surface. The increase in impedance after aptamer immobilization on the Sulfo-SMCC-modified electrode is due to decreased diffusion and changes in charge transfer kinetics at the electrode surface due to the presence of immobilized aptamers. The decrease in anodic and cathodic CV peaks after aptamer immobilization indicates a decrease in the accessibility of the electrode's active sites due to the presence of bound aptamers, which could hinder the electrochemical reactions occurring at the interface. Following these steps, the electrodes were ready for SPSFQ protein binding. In the final stage, blocking was achieved by incubating with 6-MCH for 30 min. Changes in surface conductivity and electron transfer ability following 6-MCH application were confirmed by CV measurements and EIS spectra (Fig. 6). Optimization studies were conducted by impedimetrically determining the binding abilities of the functionally configured electrodes to SPSFQ protein at different concentrations.

Surface characterization of the biosensor

SEM and AFM methods were used to examine the surface morphology of the SPSFQ aptasensor at different immobilization stages. AFM analyses were performed in non-contact mode and on a 5 × 5 μm area. SEM and AFM images of the bare ITO-PET electrode surface (Fig. 7A) show a homogeneous morphology. After OH activation, a homogeneous distribution of features is evident (Fig. 7B). Following 3-APTES application, the AFM cross-sectional view reveals increased voids, indicating that the silane agent has interacted with the –OH groups on the electrode surface (Fig. 7C). Following OH activation, a clear change in surface morphology is observed with SEM after the application of 3-APTES. Compared to the 3-APTES modification

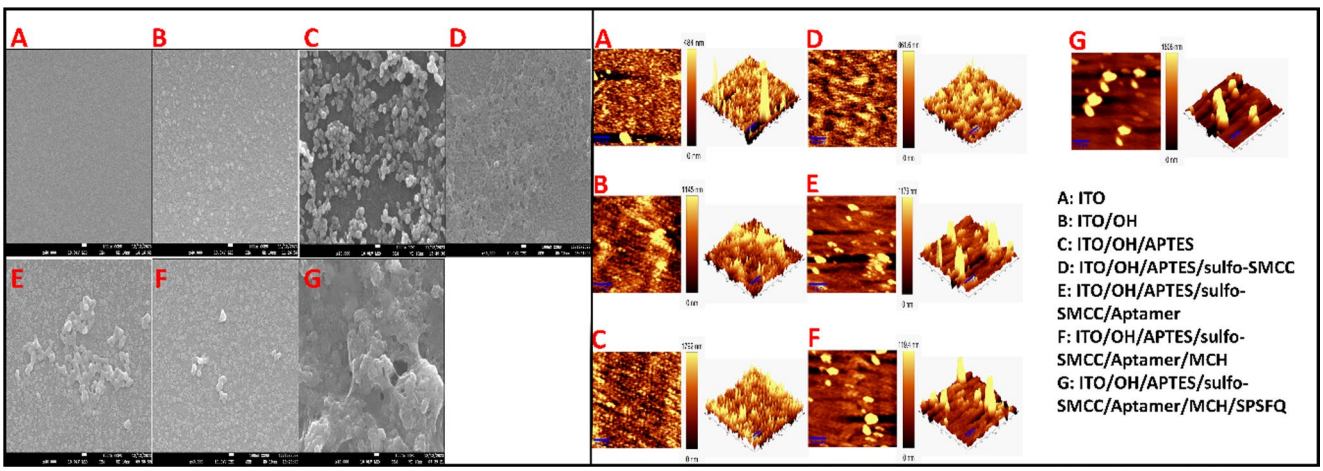


Fig. 7 SEM and AFM images of the bare ITO-PET electrode (**A**) hydroxylated ITO-PET electrode (**B**). 3-APTES modified electrode surface (**C**), sulfo-SMCC-modified electrode surface (**D**) SPSFQ aptamer-immobilized electrode surface (**E**), 6-MCH blocked electrode surface (**F**) and surface characteristics after interaction of SPSFQ with SPSFQ aptamer (**G**)

stage, softer edges and increased voids in the sulfo-SMCC-applied stage indicate changes in surface morphology. In the next modification stage, the application of sulfo-SMCC, a heterobifunctional crosslinking agent, appears to result in a homogeneous layer of surface coverage (Fig. 7D). The roughness values obtained in the AFM stage are given in Table S8. In AFM analysis, SA represents the average surface roughness, while SQ corresponds to the root mean square (RMS) surface roughness. The APTES modification stage significantly increased the surface roughness (SA: 443.053 nm, SQ: 515.806 nm). This increase in roughness indicates successful modification and likely a higher amino group density on the surface. The decrease in roughness in the sulfo-SMCC stage supports the formation of a more compact or uniform layer on the surface due to the cross-linking properties of sulfo-SMCC. This finding is also consistent with the SEM image. It was determined that the aptamer binding step caused an increase in surface roughness compared to the previous step (SA: 289.51 nm, SQ: 336.909 nm), indicating successful aptamer binding to the surface (Fig. 7E). A decrease in roughness was observed during the 6-MCH application step. This decrease can be explained by 6-MCH filling the voids or providing a smoother layer on the immobilized aptamers (Fig. 7F). The change in surface morphology following aptamer binding was also confirmed by SEM images. The successful binding of the SPSFQ protein to the aptamer-functionalized biosensor is evident from the change in surface morphology (Fig. 7G). The significant increase in AFM surface roughness and cross-sectional data, consistent with SEM, indicate successful binding of protein. The surface morphology data are consistent with the EIS and CV data, supporting the finding that the aptasensor was successfully developed.

Optimization studies

All optimization studies were conducted using SPSFQ protein concentrations in the range of 1.0–10,000 fg/mL. OH-activated ITO-PET electrodes were incubated overnight with 1% and 2% 3-APTES, while other parameters were kept constant. Although the graphical data obtained with the 1% and 2% APTES applications were similar, this value was selected in the subsequent optimization stage because the 2% APTES application was found to extend the measurement range and increase signal stability. Increasing the APTES concentration from 1% to 2% appears to positively impact biosensor performance by increasing surface modification, improving subsequent layer adhesion, and potentially increasing sensitivity and signal strength.

Optimizing the sulfo-SMCC concentration in electrochemical EIS biosensors is critical for the controlled and effective immobilization of biomolecules. This optimization directly affects the biomolecule binding efficiency, specificity, stability, and homogeneity, contributing to the sensitivity, selectivity, and reliability of the biosensor in detecting the target analyte. In this context, while other parameters were kept constant, sulfo-SMCC concentrations were determined as 0.05, 0.1, and 0.2 mM, respectively, and their effects on the biosensor response were investigated. Impedimetric measurements were performed by incubating the resulting biosensor with SPSFQ protein in the 1.0 fg/mL − 10,000 fg/mL range for 1 h. As seen in Fig. S2, it was determined that the linear relationship between the variables was strengthened in experiments where the sulfo-SMCC concentration was 0.2 mM. Increasing the sulfo-SMCC concentration to 0.2 mM facilitated effective surface functionalization of the biosensor. This effect of sulfo-SMCC can be attributed to more efficient binding of thiol-modified aptamers and improved biosensor ability to capture and detect SPSFQ protein. Therefore, configuring the biosensor with 0.2 mM sulfo-SMCC was deemed appropriate for ongoing optimization studies.

To determine the effect of aptamer concentration on biosensor performance, biosensors were configured with aptamer concentrations of 0.5 µM and 1 µM, keeping other parameters constant. The optimization step revealed that the highest regression coefficient and widest linear range were obtained at 1 µM aptamer concentration. It is anticipated that better coverage of the aptamer-modified electrode surface results in more effective immobilization of aptamers on the surface, resulting in a greater number of binding sites for the analyte. This concentration likely contributed to the observed improvements in biosensor performance by providing a favorable balance between surface coverage, binding capacity, and aptamer accessibility. Optimization studies revealed a linear relationship for the biosensor over a wide range between 1.0 fg/mL and 10,000 fg/mL. This range corresponds to a molar concentration of approximately 0.028 fM and 280 fM.

Analytical characterization of biosensor

Construction of the calibration curve

The calibration curve of the aptamer-based EIS biosensor is essential for evaluating its sensitivity and defining the linear detection range for the target analyte, the SPSFQ protein. The calibration curve illustrates the relationship between SPSFQ protein concentration (1.0–10,000 fg/mL) and the electrochemical parameter ΔRct (change in charge transfer resistance). The linear relationship between ΔRct values in the calibration curve over the concentration range of 1.0–10,000 fg/mL demonstrates that the biosensor can perform

reliable measurements over this wide range. The resulting calibration curve is shown in Fig. 8A.

Reproducibility studies

The graph of the reproducibility study conducted with 10 different calibration curves is shown in Fig. 8B. The % RSD value obtained from these data was found to be 6.62%. The equations and R^2 values of the reproducibility graphs are shown in Table S9. The developed aptasensor demonstrates exceptionally good reproducibility. R^2 values above 0.99 for all graphs indicate a near-perfect fit to the linear model, demonstrating high reliability. The narrow slope variation indicates consistent aptasensor operation and is unaffected by small deviations in measurement conditions. This demonstrates the aptasensor's excellent sensitivity and accuracy. Overall, the developed aptasensor offers strong reproducibility for both research and real sample applications.

Repeatability studies

By applying 2000 fg/mL SPSFQ protein to 10 different electrodes independently, the corresponding concentrations for each electrode were calculated from the equation of the linear calibration curve (y = 0.7855x + 332.88). The average value of the obtained data set was calculated as 2023.76 ± 53.01 fg/mL. The percentage variation value calculated using the data set was found to be 2.62%. The average value of the obtained data is quite close to the applied target concentration of 2000 fg/mL. This indicates that the biosensor measured very close to the accuracy and operated in accordance with the modeling equation. The relatively low standard deviation indicates that there was no large deviation between measurements and that the sensors exhibited consistent performance. A variation of 2.62% indicates that the biosensor's accuracy is very good, given that a typical acceptable variation in biomedical measurements is about 5% [26]. A variation below 5% supports the biosensor's high repeatability and accuracy. The agreement between the mean and target values supports the finding that both the sensor's calibration accuracy and measurement precision are strong.

Determination of LOD and LOQ values

LOD and LOQ are the minimum concentrations measured and quantified. The 3 σ/m and 10 σ/m equations were used to determine LOD and LOQ. The calculated LOD and LOQ values derived from these equations were 5.44 fg/mL and 18.15 fg/mL, respectively. The amount of SPSFQ,

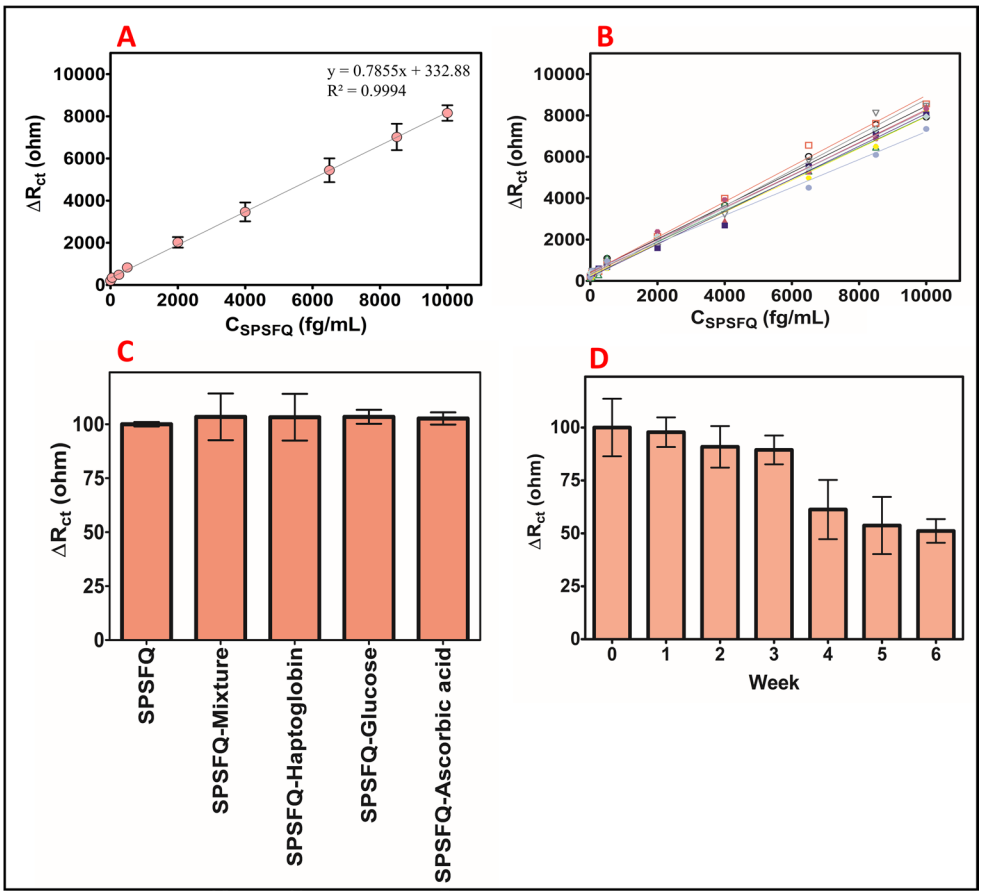


Fig. 8 **A**) Linear calibration curve of the developed SPSFQ aptasensor, **B**) linear graphs of reproducibility studies, **C**) graph of selectivity and D) graph of storage stability

a secretory protein, is closely correlated with the presence of *A. baumannii*. Studies with other pathogens have shown that secretory protease can be secreted at levels of µg/mL in the presence of 10^8–10^9 cfu/mL of pathogens [27]. Given that the biosensor developed in this study exhibits linear behavior across very low analyte ranges, it is anticipated that it can indirectly detect the presence of *A. baumannii* even at very low cfu/mL concentrations. There are aptamer sequences developed directly for *A. baumannii* in the literature, although not for secretory proteins. In different studies conducted with ssDNA aptamers selected for *A. baumannii*, electrochemical-based aptasensors with very low detection limits were developed [28, 29]. While aptasensor studies using ssDNA aptamers have focused on the direct detection of *A. baumannii* cells at very low concentrations, the current work advances this approach by targeting SPSFQ, a secretory protein strongly associated with the bacterial entity, thus enabling an indirect yet highly sensitive identification strategy that expands the scope of biosensors for diagnosis. Moreover, the ability to detect SPSFQ at fg/mL levels suggests that the biosensor can reveal bacterial activity at an earlier stage than conventional cell-based assays.

Determination of the biosensor selectivity

Figure 8C shows the column graph of the impedimetric changes obtained by applying the interferents haptoglobin, glucose, and ascorbic acid at a concentration of 250 fg/mL to the electrodes, both independently and in combination with 250 fg/mL SPSFQ protein. The SPSFQ-specific aptamer can selectively recognize both the three-dimensional structure and chemical properties of the target molecule, supporting the high specificity of the biosensor. It was determined that the interfering molecules caused only minimal changes in the signal. When the %ΔRct change obtained with the SPSFQ protein was assumed as 100, interference values were calculated as 3.23% for haptoglobin, 3.41% for the mixture, 3.42% for glucose, and 2.65% for ascorbic acid.

Storage life of the biosensor

The storage stability of the aptasensor was evaluated over a 6-week period (Fig. 8D). The relative response decreased gradually from 100% at week 0 to 97.81% at week 1, 90.90% at week 2, and 89.45% at week 3. A more pronounced decline was observed from week 4 onward, with responses dropping to 61.28% at week 4, 53.72% at week 5, and 51.15% at week 6. These results indicate that the aptasensor retained acceptable functionality for up to three weeks with minimal loss of activity (< 11%), while a substantial decrease in performance occurred after the fourth week. Consequently, the effective storage lifetime of the aptasensor can be considered to be approximately three weeks under the tested conditions.

Table 1 Data obtained from the application of SPSFQ protein at different concentrations to a commercial real human serum sample

Concentration of SPSFQ added to serum (fg/mL)	SPSFQ concentrations (fg/mL) calculated from the calibration graph	% recovery ($n=3$)	% RSD
250	277.11 ± 34.59	110.84%	12.48%
6500	6786.24 ± 106.39	104.40%	1.57%

Determination of SPSFQ protein in commercial human serum samples

Commercial human serum samples were spiked independently to achieve final SPSFQ concentrations of 250 fg/mL and 6500 fg/mL. Data obtained from the serum samples are shown in Table 1.

As seen in Table 1, the measured values are very close to the spiked SPSFQ concentrations, although some deviation is observed at each level. The recovery obtained for the 250 fg/mL SPSFQ addition was calculated as 110.84%. This may be due to the low signal-to-noise ratio (SNR) at low concentrations. Accuracy deviations may occur as the sensor approaches the LOD. The % RSD value of 12.48% indicates that repeatability is lower than that obtained with the 6500 fg/mL addition. For the 6500 fg/mL addition, % recovery was calculated as 104.40%, indicating that the sensor offers very high accuracy at this concentration. The % RSD value of 1.57% obtained with the 6500 fg/mL addition indicates that the sensor provides excellent reproducibility at high concentrations. This demonstrates that the sensor operates reliably even at the upper limit of its dynamic range. At high concentrations, both accuracy (4.40% deviation) and repeatability (1.57% RSD) are quite good. This demonstrates that the sensor offers reliable performance at high concentrations. At lower concentrations, accuracy and repeatability decrease. This is to be expected when the sensor's sensitivity limits are approached. While performance degradation is observed at low concentrations, overall the sensor exhibits good accuracy and reproducibility in real serum samples. Aptamers offer high specificity and binding affinity to target proteins. However, complex serum components can reduce specific binding by restricting the aptamer's access to the analyte. This can negatively impact binding kinetics, particularly at low analyte concentrations. The natural ionic strength and pH of serum can affect the aptamer's structural stability and binding kinetics. These factors can reduce measurement sensitivity, especially at relatively low concentrations. At 6500 fg/mL, matrix effects are thought to be less pronounced at this concentration, and binding to the target protein, SPSFQ, becomes more

dominant. The low % RSD (1.57%) obtained at 6500 fg/mL indicates that the aptamer binds the target very specifically at higher concentrations and discriminates well between the target and other molecules.

Conclusion

This work reports the first selection of DNA aptamers against the *A. baumannii* SPSFQ protein and their successful integration into an EIS biosensor for SPSFQ detection. The aptamers showed high affinity for SPSFQ (nanomolar Kd values), confirming their strong binding interaction with the target. The wide dynamic range (1.0–10,000 fg/mL) and very low detection (LOD = 5.44 fg/mL) and quantification (LOQ = 18.15 fg/mL) limits obtained from the calibration curve demonstrate that the biosensor can reliably measure ultra-low analyte concentrations. Minimal cross-reactivity was observed in selectivity tests, confirming that the aptamer binds strongly to SPSFQ and that potential interferents do not significantly affect the sensor's performance. These findings confirm the biosensor's reliable and selective performance in detecting SPSFQ within complex biological matrices, with particular applicability to commercial human serum. Together, these findings underscore the strong analytical performance of the biosensor and introduce the first aptamer-based recognition strategy for the *A. baumannii* SPSFQ protein. Accordingly, the developed biosensor represents a promising tool for early detection and monitoring in clinical applications. The indirect detection strategy used in this study is based on the assumption that SPSFQ is a secretory protease produced by *A. baumannii* and that its presence reflects bacterial activity. Although previous studies on bacterial pathogens have shown that secreted protease levels correlate with bacterial cell density, the present study focuses on evaluating the feasibility and analytical performance of SPSFQ detection rather than establishing a direct quantitative relationship between SPSFQ concentration and *A. baumannii* CFU/mL. Establishing such correlations (e.g., between SPSFQ levels and *A. baumannii* counts in culture supernatants) will be an important objective for future studies aimed at clinical applications. Furthermore, the SPSFQ-specific aptamers generated in this study represent promising recognition elements for a wide range of diagnostic platforms directed toward *A. baumannii* detection.

Supplementary Information The online version contains supplementary material available at https://doi.org/10.1007/s00604-026-07866-2.

Acknowledgements This work was supported by the Scientific and Technological Research Council of Turkey (TÜBİTAK) under Project No. 221Z345.

Author contributions C.Ö.: Conceptualization, all experimental studies, funding acquisition, investigation, formal analysis, data curation, writing—original draft preparation, and review and editing.M.A.: EIS experimental studies.G.Ü.: SELEX experimental studies.E.M.: SELEX experimental studies.S.E.: Conceptualization, review and editing.M.K.S.: Conceptualization, review and editing.

Funding Open access funding provided by the Scientific and Technological Research Council of Türkiye (TÜBİTAK). Scientific and Technological Research Council of Turkey (TÜBİTAK) [grant number 221Z345].

Data availability This manuscript does not report data generation or analysis.

Declarations

Competing interests The authors declare no competing interests.

Open Access This article is licensed under a Creative Commons Attribution 4.0 International License, which permits use, sharing, adaptation, distribution and reproduction in any medium or format, as long as you give appropriate credit to the original author(s) and the source, provide a link to the Creative Commons licence, and indicate if changes were made. The images or other third party material in this article are included in the article's Creative Commons licence, unless indicated otherwise in a credit line to the material. If material is not included in the article's Creative Commons licence and your intended use is not permitted by statutory regulation or exceeds the permitted use, you will need to obtain permission directly from the copyright holder. To view a copy of this licence, visit http://creativecommons.org/licenses/by/4.0/.

References

1. Kumar S, Anwer R, Azzi A (2021) Virulence potential and treatment options of multidrug-resistant (MDR) *Acinetobacter baumannii*. Microorganisms 9:2104. https://doi.org/10.3390/microorganisms9102104
2. Monem S, Furmanek-Błaszk B, Łupkowska A, Kuczyńska–Wiśnik D, Stojowska–Swędrzyńska K, Laskowska E (2020) Mechanisms protecting *Acinetobacter baumannii* against multiple stresses triggered by the host immune response, antibiotics, and outside–host environment. Int J Mol Sci 21:5498. https://doi.org/10.3390/ijms21155498
3. Yehya A, Ezzeddine Z, Chakkour M, Dhaini H, Bou Raad R, Ghssein G (2025) The intricacies of *Acinetobacter baumannii*: a multifaceted comprehensive review of a multidrug-resistant pathogen and its clinical significance and implications. Front Microbiol 16:1565965. https://doi.org/10.3389/fmicb.2025.1565965
4. Bagudo AI, Obande GA, Harun A, Singh KKB (2020) Advances in automated techniques to identify *Acinetobacter calcoaceticus–Acinetobacter baumannii* complex. Asian Biomed 14:177–186. https://doi.org/10.1515/abm-2020-0026
5. Hu WW, He JW, Guo SL, Li J (2022) Development and evaluation of a rapid and sensitive multienzyme isothermal rapid amplification with a lateral flow dipstick assay for detection of *Acinetobacter baumannii* in spiked blood specimens. Front Cell Infect Microbiol 12:1010201. https://doi.org/10.3389/fcimb.2022.1010201

6. Bahari D, Babamiri B, Salimi A, Salimizand H (2021) Ratiometric fluorescence resonance energy transfer aptasensor for highly sensitive and selective detection of *Acinetobacter baumannii* bacteria in urine sample using carbon dots as optical nanoprobes. Talanta 221:121619. https://doi.org/10.1016/j.talanta.2020.121619
7. Cheng X, Yang J, Wang M, Wu P, Du Q, He J, Tang Y (2019) Visual and rapid detection of *Acinetobacter baumannii* by a multiple cross displacement amplification combined with nanoparticles-based biosensor assay. AMB Express 9:30. https://doi.org/10.1186/s13568-019-0754-0
8. Cao L, Wang T, Xie J, Wang Y, Huang Y, Luo S, Zhan X, Jiang H, Ran L, Jin X, Liu J, Li B (2025) Aptamer-based DNAzyme walker electrochemical biosensing strategy for *Acinetobacter baumannii* detection. Bioelectrochemistry 163:108895. https://doi.org/10.1016/j.bioelechem.2024.108895
9. Wang Y, Huang Y, Zhang Y, Wang H (2025) Ultrasensitive detection of staphylococcal enterotoxin B using electrochemical nanoprobe based on AgNPs@para-sulfonatocalix[4]arene-functionalized MXene. Sens Actuators B Chem 426:137126. https://doi.org/10.1016/j.snb.2024.137126
10. Patel S (2017) A critical review on serine protease: key immune manipulator and pathology mediator. Allergol Immunopathol (Madr) 45:579–591. https://doi.org/10.1016/j.aller.2016.10.011
11. Borberg E, Granot E, Patolsky F (2022) Ultrafast one-minute electronic detection of SARS-CoV-2 infection by 3CLpro enzymatic activity in untreated saliva samples. Nat Commun 13:6203. https://doi.org/10.1038/s41467-022-34074-2
12. Muhammed NS, Hussin N, Lim AS et al (2021) Recombinant production and characterization of an extracellular subtilisin-like serine protease from *Acinetobacter baumannii* of fermented food origin. Protein J 40:419–435. https://doi.org/10.1007/s10930-021-09986-5
13. Elskens JP, Elskens JM, Madder A (2020) Chemical modification of aptamers for increased binding affinity in diagnostic applications: current status and future prospects. Int J Mol Sci 21:4522. https://doi.org/10.3390/IJMS21124522
14. Zhang H, Sun Z, Sun K, Wang Y, Zhang Y, Wang B (2025) Electrochemical impedance spectroscopy–based biosensors for label–free detection of pathogens. Biosensors (Basel) 15:443. https://doi.org/10.3390/bios15070443
15. Hanahan D, Jessee J, Bloom FR (1991) Plasmid transformation of *Escherichia coli* and other bacteria. Methods Enzymol 204:63–113. https://doi.org/10.1016/0076-6879(91)04006-A
16. Ozyurt C, Evran S, Telefoncu A (2013) Development of a novel fluorescent protein construct by genetically fusing green fluorescent protein to the N-terminal of aspartate dehydrogenase. Biotechnol Appl Biochem 60:399–404. https://doi.org/10.1002/bab.1107
17. Bradford MM (1976) A rapid and sensitive method for the quantitation of microgram quantities of protein utilizing the principle of protein-dye binding. Anal Biochem 72:248–254. https://doi.org/10.1016/0003-2697(76)90527-3
18. Laemmli UK (1970) Cleavage of structural proteins during the assembly of the head of bacteriophage T4. Nature 227:680–685. https://doi.org/10.1038/227680A0
19. Avci-Adali M, Paul A, Wilhelm N et al (2009) Upgrading SELEX technology by using lambda exonuclease digestion for Single-Stranded DNA generation. Molecules 15(1–11):1–11. https://doi.org/10.3390/MOLECULES15010001
20. Kouhpayeh S, Hejazi Z, Khanahmad H, Rezaei A (2017) Real–time PCR: an appropriate approach to confirm SsDNA generation from PCR product in SELEX process. Iran J Biotechnol 15:143–148. https://doi.org/10.15171/ijb.1550
21. Bailey TL, Johnson J, Grant CE, Noble WS (2015) The MEME suite. Nucleic Acids Res 43:W39–W49. https://doi.org/10.1093/NAR/GKV416
22. Zuker M (2003) Mfold web server for nucleic acid folding and hybridization prediction. Nucleic Acids Res 31:3406–3415. https://doi.org/10.1093/NAR/GKG595
23. Hulme EC, Trevethick MA (2010) Ligand binding assays at equilibrium: validation and interpretation. Br J Pharmacol 161:1219–1237. https://doi.org/10.1111/J.1476-5381.2009.00604.X
24. Zhen J, Liang G, Chen R, Jia W (2020) Label-free hairpin-like aptamer and EIS-based practical, biostable sensor for acetamiprid detection. PLoS One 15:e0244297. https://doi.org/10.1371/journal.pone.0244297
25. Trunzo NE, Hong KL (2020) Recent progress in the identification of aptamers against bacterial origins and their diagnostic applications. Int J Mol Sci 21:6757. https://doi.org/10.3390/ijms21145074
26. Ivanauskas F, Katauskis P, Laurinavičius V (2014) Mathematical modeling of biosensor action in the region between diffusion and kinetic modes. J Math Chem 52:689–702. https://doi.org/10.1007/s10910-013-0289-6
27. Neddermann M, Backert S (2019) Quantification of serine protease HtrA molecules secreted by the foodborne pathogen *Campylobacter jejuni*. Gut Pathog 11:14. https://doi.org/10.1186/S13099-019-0295-8
28. Abedi R, Raoof JB, Mohseni M, Bagheri Hashkavayi A (2023) Development of a label-free impedimetric aptasensor for the detection of *Acinetobacter baumannii* bacteria. Anal Biochem 679:115288. https://doi.org/10.1016/J.AB.2023.115288
29. Geravand M, Erfani Y, Nematpour N et al (2024) Nanoarchitectonics of aptamer-based electrochemical biosensor utilizing electerospun carbon nanofibers and gold nanoparticles for *Acinetobacter baumannii* detection. Microchem J 200:110437. https://doi.org/10.1016/J.MICROC.2024.110437

Publisher's Note Springer Nature remains neutral with regard to jurisdictional claims in published maps and institutional affiliations.